INTERCEPTION OF MANEUVERING TACTICAL BALLISTIC MISSILES IN THE ATMOSPHERE

Shinar J.* and Zarkh M.**
Faculty of Aerospace Engineering
Technion, Israel Institute of Technology
Haifa,Israel.

Abstract

The paper reports the results of an extensive point-mass simulation study on the interception of a high speed reentering tactical ballistic missile (TBM) having structural asymmetries. Due to the high reentry velocity and the structural asymmetries high intensity maneuvers and roll rates may develop, generating a "barrel-roll" type trajectory. The interceptor is a generic endoatmospheric guided missile of simplified dynamics, designed for high altitude interceptions. The simulation study evaluates four different guidance laws for this purpose. It is demonstrated that the interception of a maneuvering TBM can be successful only if perfect measurements and accurate estimation of the target maneuvers are guaranteed. Without both of these features a "hit-to-kill" homing accuracy is unlikely.

Notation

a	acceleration (lateral)
a^c	acceleration command
b	TBM roll damping parameter, see (3)
c	TBM "roll asymmetry" factor, see (4)
C_D	drag coefficient
C_L	lift coefficient
C_{r0}	rolling moment coefficient due to a lateral asymmetry
C_{rp}	roll damping coefficient (< 0)
d	distance of reference
g	acceleration of gravity
h	altitude
I_{xx}	moment of inertia in roll
m	mass
n	lateral load factor, see (A-13)
N'	interceptor guidance gain
p	roll rate in body coordinates
R	range
S	surface of reference
t	time
t_b	interceptor rocket motor burning time
V	velocity
V_c	closing speed, see (A-7)
x,y	horizontal displacements
α_{tr}	TBM trimmed angle of attack
β	TBM ballistic coefficient
γ	flight path angle (in the vertical plane)
η	normalized "time-to-go", see(13)
λ	TBM trimmed lift/drag ratio
μ	missile/target maneuver ratio, see (20)
σ	line of sight angle
φ	roll angle (with respect to the horizon)
χ	heading angle (in the horizontal plane).
ψ	dynamic compensation factor, see (17)
τ	interceptor autopilot time constant
Ω	acceleration kernel, proportional to the "zero-effort miss distance"

subscripts

A	of the TBM (attack)
D	of the interceptor (defense)
f	final
h	horizontal
i,j	dummy indices
max	maximum value
v	vertical
0	initial value

---

* Max and Lottie Dresher Professor of Aerospace Performance and Propulsion, Associate Fellow AIAA.
** Senior Research Fellow, supported by the Center of Absorption in Science, Ministry of Immigrant Absorption, State of Israel.

Introduction

For many years the reentry trajectory of a tactical ballistic missile (TBM) has been assumed to be predictable. Based on this assumption intercepting a TBM seemed to be a feasible task [1], at least from the conceptual point of view, requiring mainly a quick reaction defense system. In these days, state of art technology enables one to design a guided missile for intercepting a non maneuvering TBM with an excellent homing accuracy. Moreover, even a "hit-to-kill" capability, a very desirable feature for an anti-ballistic missile defense system, can be contemplated.

Recent experience indicated, however, that the assumption of predictable TBM reentry trajectories may not be valid. These indications have raised an increasing concern of maneuvering reentry vehicles and the difficulties of their interception [2]. The present paper addresses anti-ballistic missile defense scenarios against highly maneuverable reentry vehicles. Such scenarios will become inevitable in the future, if the currently developed defense systems will be successful against non maneuvering threats [3]. As a consequence, the designers of a future TBM will have to incorporate a maneuvering capability in their weapon system in order to generate less predictable reentry trajectories and to make the interception much more difficult. The high reentry velocity of the TBM provides it with a potential of high maneuverability, which can be applied in a rather simple way by a smart designer. Thus, a TBM can be easily made as maneuverable (or even more) as the defensive missile and would be able to avoid interception. Even a random maneuver can make the reentry trajectory of a TBM unpredictable.

The predictability of a reentry trajectory has been based on the assumption that the missile is designed to be symmetrical and, - being a stable flying vehicle, - will fly at a nearly zero angle of attack. Experience with several types of flying vehicles has shown [4-5] that structural asymmetries create a non-zero trim angle of attack, as well as an induced roll rate. The effects of such asymmetries on ballistic reentry trajectories were extensively studied [6-9] to avoid catastrophic roll resonance.

A set of exploratory point-mass simulations with generic TBM models, carried out in the context of anti-ballistic missile defense, indicated that below an altitude of 20 km high intensity maneuvers may develop even for moderate longitudinal asymmetries. If such a longitudinal asymmetry is coupled with a small lateral asymmetry, a "barrel-roll" type trajectory, far away from roll resonance, is generated.

The paper reports the results of an extensive point-mass simulation study on the interception of a reentering high speed TBM with structural asymmetries by a hypothetical endoatmospheric guided missile of a simplified dynamic model. The the simulation study compares the homing performance of identical interceptor missiles using different guidance laws against a TBM performing "barrel-roll" type maneuvers.

In the next section the three-dimensional point-mass simulation model is described. It is followed by a parametric representation of characteristic reentering TBM families and the definition of the different interceptor guidance laws used in the simulation. As an example, detailed results of the interception engagements against a member of a reentering TBM family are presented and discussed.

Simulation Model

General Outline.

In order to evaluate the homing performance of a guided interceptor missile against reentering ballistic vehicles a modular three-dimensional point-mass simulation model was set up. The simulation model consists of the following elements: relative kinematics between two point-mass vehicles, point-mass dynamics of both flying vehicle, simplified guidance and control dynamics of each vehicle and a

high-altitude atmospheric model. The simulations are carried out in a fixed Cartesian coordinate system, assuming flat non rotating earth and no wind. The well known equations of three-dimensional kinematics and point-mass dynamics of an atmospheric vehicle are summarized in the Appendix. In this section the interception scenario is outlined, followed by the description of the specific guidance and control models of a maneuvering TBM and the interceptor missile.

Interception Scenario

The present study concentrates on a point defense scenario, i. e. the interceptor missile is launched from the vicinity of the TBM's target. The initial position of the TBM is determined by assuming a non maneuvering ballistic trajectory aimed at the target, which serves as the origin of the coordinate system. The initial position of the TBM also determines the vertical plane of reference ($y_i = \chi_i = 0$). When the reentering TBM is detected, the defense system selects the desired altitude for interception h^* and launches a guided missile in the vertical plane of reference towards the predicted point of impact at this altitude. Taking into consideration that the TBM may carry an unconventional warhead, the interception has to take place at a rather high altitude. In this study the range of planned interception altitudes between 20 to 26 kms is evaluated. The aerodynamic and propulsive features of the interceptor missile were designed in order to allow such interceptions.

TBM model

The reentering TBM (the attacking missile, denoted by the subscript A) is assumed to be a generic cruciform flying vehicle having some structural asymmetries. The longitudinal asymmetries of the TBM create (in stable atmospheric flight) a constant non zero trimmed angle of attack α_{tr} in body coordinates. As a consequence, a lift force, proportional to the dynamic pressure

$$L_A = 0.5\,[\rho(h)V^2\,S\,C_L(\alpha_{tr})]_A \qquad (1)$$

is generated. The lateral (anti-symmetric) asymmetries create a rolling moment, which is also proportional to the dynamic pressure, resulting in a roll rate which obeys the differential equation [10]

$$\dot{p}_A + b\,\rho(h_A)V_A p_A = c\,\rho(h_A)V_A^2 \qquad (2)$$

where the parameters "b" and "c" are

$$b = -0.25\,(S\,d^2\,C_{rp} / I_{xx})_A > 0 \qquad (3)$$

$$c = 0.5\,(S\,d\,C_{r0} / I_{xx})_A \qquad (4)$$

"b" being a measure of the aerodynamic damping in roll and "c" is a measure of the anti-symmetric "roll asymmetry". The roll angle of the TBM φ_A is obtained by integrating $\dot{\varphi}_A$, given by [10]

$$\dot{\varphi}_A = p_A + \dot{\chi}_A \sin\gamma_A \qquad (5)$$

from a given initial condition φ_{A0}.

Any member of the generic TBM family used in this study is characterized by the ballistic coefficient,

$$\beta = (m/S\,C_D)_A \qquad (6)$$

which determines the deceleration in the atmosphere, the lift to drag ratio at the non zero trimmed angle of attack α_{tr},

$$\lambda = [C_L(\alpha_{tr}) / C_D]_A \qquad (7)$$

which serves as a measure of longitudinal asymmetry, as well as the parameters "b" and "c" defined in (3) and (4).

Having no thrust, the TBM point-mass simulation model {see eqs.(A-10)-(A-12)} has only 3 inputs: the aerodynamic forces L_A and D_A and the roll angle φ_A.

The initial conditions of reentry are specified at the altitude of 150 km. For one of the examples used in the simulation

study, Fig. 1. shows the velocity, the lateral load factor and the roll rate of the TBM as a function of altitude below 40 km, based on the data given in Table 1.

Table 1. TBM Example Data.

$V_{A0} = 2.2$ km/s	$\gamma_{A0} = -40$ deg
$\beta = 5000 kg/m^2$	$\lambda = 2.82$
$b = 0.004\ m^2/kg$	$c = 3.3\ 10^{-6}$ m/kg

Interceptor Model

This interceptor missile (of the defense system, denoted by the subscript D) has an aerodynamically controlled cruciform airframe which is roll stabilized. In order to allow high altitude endoatmospheric interceptions it has a two stage solid rocket propulsion. Each rocket motor provides a constant thrust. After the first stage separation occurs and the rocket motor of the second stage is ignited. The maneuverability of the missile (its lateral acceleration and the corresponding load factor) is limited, in each of the two perpendicular planes of the cruciform configuration (j= 1,2) by the maximum lift coefficient.

$$(n_D)_j \le 0.5\,[\rho(h) V^2 S\, C_{Lmax} / g\, m]_{Dj} \qquad (8)$$

The thrust, lift, drag and other interceptor parameters are summarized in Table 2.

Table 2. Interceptor Data.

Stage	1	2
t_b [sec]	6.5	13.0
T [kN]	229	103
m_0 [kg]	1540	781
m_f [kg]	933	236
SC_D [m^2]	0.40	0.20
SC_{Lmax} [m^2]	0.24	0.20

The guidance system of the interceptor missile consists of two identical, fully decoupled channels, associated with the perpendicular planes of the cruciform configuration. Since the missile is roll stabilized, one channel is designated to perform lateral accelerations in the vertical plane (j=1=v),

$$(a_D)_v = g\,(n_D)_v \triangleq g\, n_D \cos\varphi_D \qquad (9)$$

and the other in the horizontal plane (j=2=h).

$$(a_D)_h = g\,(n_D)_h \triangleq g\, n_D \sin\varphi_D \qquad (10)$$

For sake of simplicity it is assumed that the missile has an ideal (noise free) seeker and an autopilot represented by a first-order transfer function. Therefore, the relationship between the acceleration command of the interceptor in each guidance channel (j=v,h) and the respective lateral acceleration is given by

$$(a_D)_j = [(a_D^c)_j - (a_D)_j] / \tau \qquad (11)$$

The time constant τ represents an approximation of the closed loop autopilot dynamics. This time constant is a function of the actual flight conditions (speed and altitude) and increases as the dynamic pressure is reduced. Interceptor velocity, the maximum lateral load factor of each guidance channel and the autopilot time constant, computed along a trajectory for intercepting a reentering TBM at $h^* = 23$ km, are plotted in Fig. 2 as function of altitude.

The acceleration command for each channel is generated by the appropriate missile's guidance law. In the present study four different guidance laws, all expressible by a similar mathematical structure,

$$(a_D^c)_j = N' \Omega_j(\eta) \qquad (12)$$

are compared. In (12) η is the normalized "time-to-go" defined by

$$\eta \triangleq (t_f - t)/\tau \qquad (13)$$

N' is the (eventually time dependent) guidance gain and $\Omega_j(\eta)$, having the dimensions of acceleration, is a *kernel* proportional to the so-called "zero-effort miss distance" according to the assumptions of the particular guidance law concept. The guidance laws considered in this study are:

(i) "Classical" proportional navigation (PN) with a constant effective gain [11].

$$[\Omega_j(\eta)]_{PN} = V_c \dot{\sigma}_j, \qquad (N')_{PN} = 4 \qquad (14)$$

(ii) Augmented proportional navigation (APN), assuming known (or accurately measured) target acceleration [12].

$$[\Omega_j(\eta)]_{APN} = [\Omega_j(\eta)]_{PN} + 0.5(a_A)_j \qquad (N')_{APN} = 3 \qquad (15)$$

(iii) Optimal guidance law (OGL) with time-varying gain, based on known target acceleration and compensating for own dynamics [13].

$$[\Omega_j(\eta)]_{OGL} = [\Omega_j(\eta)]_{APN} - \psi(\eta)\,(a_D)_j, \qquad (N')_{OGL} = N'(\eta) \qquad (16)$$

The dynamic compensation factor $\psi(\eta)$ is

$$\psi(\eta) = (e^{-\eta} + \eta - 1)/\eta^2 \qquad (17)$$

and the time dependent guidance gain is

$$N'(\eta) = 6\eta^4 \psi(\eta) / \{3 + 6\eta - 6\eta^2 + 2\eta^3 - 12\eta e^{-\eta} - 3e^{-2\eta}\} \qquad (18)$$

(iv) Suboptimal guidance law (SGL), similar to OGL, but without target acceleration input.

$$[\Omega_j(\eta)]_{SGL} = [\Omega_j(\eta)]_{OGL} - 0.5(a_A)_j, \qquad (N')_{SGL} = N'(\eta) \qquad (19)$$

The idea not to include target acceleration explicitly in the guidance law is based on a differential game approach and in this respect (19) can be considered as a linear approximation of the non-linear guidance law proposed in [14].

Simulation Results

A very large number of interception simulations were carried out against the members of a TBM family with different parameters (β,λ,b,c) and initial conditions (V_{A0}, γ_{A0}). Against each TBM trajectory sets of four anti-ballistic missiles with different guidance laws (PN, APN, OGL, SGL) were launched, each set being aimed to intercept the target at the same altitude.

Effect of Initial Roll Angle. The actual reentry trajectory of the TBM depends not only on the altitude profiles of its maneuverability and roll rate, but also on the initial value of the roll angle φ_{A0}, measured between the plane of maneuver (generated by the longitudinal asymmetry of the TBM) and the horizontal reference. It was found at the early stage of the study that the miss distance exhibited a high sensitivity to this initial condition. The periodical effect of this initial "phase angle" (a random variable from the anti-ballistic defense point of view) on the miss distance is illustrated in Fig. 3 for one of the simulation examples. Due to this phenomenon, in all the tested combinations of different TBM models, guidance laws and planned interception altitudes, a set of 36 simulations (for the range of $0 \geq \varphi_{A0} \geq 2\pi$) were carried out. From the ensemble of the results obtained in each case the maximum value of the miss distance, its average ("mean") value as well as the corresponding standard deviation can be computed as the relevant outputs for comparison.

Parametric Investigation

Concentrating on a TBM having the same initial reentry conditions and ballistic coefficient as in Table 1., a parametric investigation, varying the roll parameters "b" and "c", as well as the trimmed lift/drag ratio "λ", was carried out. Note, that since the simulations deal with generic vehicles and simplified dynamic models, the numerical results have only relative merits and the essential part of the analysis is qualitative.

Effect of Roll Parameters. The roll rate profile of a TBM (as shown in Fig 1.) is uniquely determined by the parameters "b" and "c". The value of "b" effects the altitude where the roll rate becomes maximal, as it can be seen in Fig. 4. For a given value of "b" the actual roll rate at any altitude is linearly proportional to "c".

Keeping the value of "b" as in Table 1., the effect of the roll rate on the the guidance laws homing performance was evaluated. In Figs. 5 and 6 the average miss distances are plotted as the function of the roll rate.

Effect of TBM Maneuverability. It is well known that the homing accuracy of a guided missile is strongly effected by the missile/target maneuver ratio "μ" in the end-game. This parameter

$$\mu \triangleq (a_D)_{max} / (a_A)_{max} \qquad (20)$$

is depicted in Fig. 7 as the function of the interception altitude for different values of "λ". This parameter (inversly proportional to "λ") has it maximum at h=22 km where interceptor's lateral acceleration becomes maximal. The maximum miss distance obtained at the planned interception altitude of $h^* = 22$ km by each guidance law against different TBM maneuverability levels, but with the same roll parameters (as given in Table 1.), is plotted in Fig. 8 as the function of "μ". The merit of each guidance law is directly determined from this figure.

Effect of Interception Altitude. Summary of detailed simulation results, namely the maximum, the "mean" value and the standard deviation (SD) of the miss distance ensembles, obtained against the TBM model presented in Fig. 1, are summarized in Table 3 as the function of the planned interception altitude h^*. It is not surprising to observe that, for all the guidance laws considered for comparison, the interception altitude with the smallest miss distance is at the neighborhood of 23 km, near to the altitude where "μ" is maximal.

Table 3. Miss Distance Summary (meters)

a. PN (N'=4)

h^* (km)	Max	Mean	SD
20	21.01	13.19	4.99
21	16.73	10.10	4.36
22	12.97	7.84	3.49
23	10.78	6.77	3.05
24	10.78	7.03	3.04
25	11.55	7.51	3.12
26	11.88	7.86	3.07

b. APN (N'=3)

h^* (km)	Max	Mean	SD
20	13.91	8.98	3.51
21	11.94	7.39	3.01
22	9.91	5.97	2.62
23	7.96	4.94	2.15
24	7.72	4.95	2.16
25	9.15	5.51	2.41
26	10.06	5.90	2.53

c. OGL

h^* (km)	Max	Mean	SD
20	0.14	0.06	0.03
21	0.10	0.06	0.03
22	0.10	0.05	0.03
23	0.11	0.06	0.03
24	0.15	0.08	0.04
25	0.18	0.11	0.04
26	0.22	0.15	0.05

d. SGL

h^* (km)	Max	Mean	SD
20	11.84	6.20	3.39
21	8.17	3.64	2.61
22	5.21	2.13	1.69
23	4.34	1.86	1.42
24	4.38	1.97	1.43
25	4.39	2.11	1.43
26	4.63	2.26	1.44

Discussion

The "barrel roll" type trajectory of the TBM, generated by longitudinal as well as lateral asymmetries, is a combination of a monotonically increasing lateral load factor n_A and roll rate $\dot{\varphi}_A$, representing a time varying lateral acceleration vector in amplitude and direction. Though such evasive maneuver is not optimal in a theoretical sense [14], it seems to be very demanding for a guided missile, as it is confirmed by a recently published paper [15] on the homing performance of an air-to air missile against an aircraft performing high-*g* barrel roll (HGB) maneuvers. In spite the differences (subsonic target speed, a rather high missile/target maneuver ratio ($\mu = 4.29$), a *horizontal* barrel roll generated by *constant* lateral acceleration and roll rate, etc.), [15] has many common elements with the present study. The paper demonstrates that, even in this relatively favorable conditions for the interceptor, HGB is a very effective evasive maneuver against PN and APN guided missiles. A periodical variation of the miss distance as a function of "time-to-go", similar to the effect of φ_{A0} illustrated in Fig. 3, is also exhibited.

The "barrel roll" type reentry trajectory of a TBM, due to structural asymmetries, is only one of the eventual difficulties that may be encountered in future anti-ballistic missile defense. It seems to serve, however, a relevant example for the analysis of such interception scenarios for the following reasons: (i) The asymmetries can be easily introduced by the TBM designer. (ii) The resulting maneuver is very demanding for the interceptor missile. The actual values of the asymmetries and the initial conditions of the reentry are random variables from the defense point of view. TBM maneuver potential being quite large, the missile/target maneuver ratio may turn out to be much smaller than the values encountered in "classical" air-to-air or surface-to-air scenarios.

Since a TBM may carry an unconventional warhead, the defense analysis has to be based on "worst case" assumptions. Thus, an effective interceptor guidance law for anti-ballistic missile defense has to minimize the maximum expected miss distance and to allow, if it is possible, a "hit-to-kill" accuracy. Due to the inherent limitations of a point-mass simulation, only very small miss distances (certainly less than 1 m) can be considered to satisfy this requirement.

Conclusions

From the results of the simulation study the following conclusions can be drawn:

1, Neither PN, nor APN seem to be adequate to intercept a maneuvering reentry vehicle. This conclusion is clearly confirmed by the result of an independent investigation [15].

2, OGL is the only guidance law with a "hit-to-kill" potential against a highly maneuvering TBM in an endoatmospheric interception. However, even in the assumed ideal *perfect information* environment, a clear maneuverability advantage (of at least 1.6-1.7) is required.

3, SGL has a much better performance than PN or APN, but only with a high maneuver advantage ($\mu > 4$) can it approach the homing accuracy required for "hit-to-kill".

4, The last two statements lead to conclude, that in a defense scenario against highly maneuvering ballistic missiles "hit-to-kill" accuracy is not feasible without accurate estimation of the actual TBM accelerations and its incrporation in the guidance law.

The results of the described simulation study are "optimistic" from the defense point of view. They are based on a simplified interceptor model, as well as on the assumptions of an ideal target detection capability and a clear maneuverability advantage of the interceptor missile. Moreover, for OGL an accurate and instantaneous estimation of the TBM acceleration is assumed. Therefore the conclusions, in particularly the last one, present a great challenge to the anti-ballistic missile defense community.

Appendix: Equations of Motion

Relative Kinematics

The motion a point-mass body (designated by a subscript i) in a Cartesian coordinate system can be defined by the magnitude of the respective velocity vector V_i and its direction in the vertical and horizontal planes respectively, described by γ_i and χ_i.

$$\dot{x}_i = V_i \cos\gamma_i \cos\chi_i \qquad \text{(A-1)}$$

$$\dot{y}_i = V_i \cos\gamma_i \sin\chi_i \qquad \text{(A-2)}$$

$$\dot{h}_i = V_i \sin\gamma_i \qquad \text{(A-3)}$$

Integrating (A-1)-(A-3) the relative position of two moving points (i=A,D) is obtained

$$\Delta x(t) \triangleq x_A(t) - x_D(t) \qquad \text{(A-4)}$$

$$\Delta y(t) \triangleq y_A(t) - y_D(t) \qquad \text{(A-5)}$$

$$\Delta h(t) \triangleq h_A(t) - h_D(t) \qquad \text{(A-6)}$$

These Cartesian components determine the range vector **R**, expressed in polar coordinates by its magnitude R and the line of sight angles σ_v and σ_h in the vertical and horizontal planes. Relative kinematics can be therefore expressed by

$$\begin{aligned}\dot{R} \triangleq -V_c = V_A\{&\cos\sigma_v \cos\gamma_A \cos(\chi_A-\sigma_h) \\ &+ \sin\sigma_v \sin\gamma_A\} \\ -V_D\{&\cos\sigma_v \cos\gamma_D \cos(\chi_D-\sigma_h) \\ &+ \sin\sigma_v \sin\gamma_D\}\end{aligned} \qquad \text{(A-7)}$$

$$\begin{aligned}\dot{\sigma}_v = [V_A\{&\cos\sigma_v \sin\gamma_A \\ &- \sin\sigma_v \cos\gamma_A \cos(\chi_A-\sigma_h)\} \\ -V_D\{&\cos\sigma_v \sin\gamma_D \\ &- \sin\sigma_v \cos\gamma_D \cos(\chi_D-\sigma_h)\}]/R\end{aligned} \qquad \text{(A-8)}$$

$$\begin{aligned}\dot{\sigma}_h = [V_A\{&\cos\gamma_A \sin(\chi_A-\sigma_h)\} \\ -V_D\{&\cos\gamma_D \sin(\chi_D-\sigma_h)\}]/R\cos\sigma_v\end{aligned} \qquad \text{(A-9)}$$

Point-Mass Dynamics

Application of the second law of Newton to each flying vehicle (i=A,D), assuming that the thrust is aligned with the velocity vector, leads to differential equations for V_i, γ_i and χ_i.

$$\dot{V}_i = [(T - D)/m - g\sin\gamma]_i \qquad \text{(A-10)}$$

$$\dot{\gamma}_i = g\,[(n\cos\varphi - \cos\gamma)/V]_i \qquad \text{(A-11)}$$

$$\dot{\chi}_i = g\,[(n\sin\varphi / V\cos\gamma)]_i \qquad \text{(A-12)}$$

the lateral load factor n_i being defined by

$$n_i = (L/g\,m)_i \qquad \text{(A-13)}$$

The aerodynamic lift and drag forces are functions of altitude and velocity

$$L_i = [\,0.5\,\rho(h)\,V^2\,S\,C_L\,]_i \qquad \text{(A-14)}$$

$$D_i = [\,0.5\,\rho(h)\,V^2\,S\,C_D\,]_i \qquad \text{(A-15)}$$

References

1. Kuroda, T. and Imado, F., "Advanced Missile Guidance System Against a Very High Speed Target", AIAA Paper 88-4092-CP, Guidance, Navigation and Control Conference, Minneapolis MN, Aug. 1988.
2, Grey, J. ,"Whither Ballistic Missile Defense?", Aerospace America, March 1994, pp. 16-21.
3. Hughes, D., "Erint Hits Storm RV Posing as Chemical Threat", Aviation Week & Space Technology, Dec 13/20, 1993, p. 57.
4. Nicolaides, J. D., "On the Free Flight Motion of Missiles Having Slight Configuration Asymmetries", US Army Ballistic Research Laboratories, Report No. 858, June 1953.
5. Murphey, C.H., "Nonlinear Motion of a Missile with Slight Configuration Asymmetries", Journal of Spacecraft & Rockets, Vol. 8, No. 3, 1971, pp. 259-263.

6. Tolosko, R.J., "Reentry Dynamics of a Trimmed Body with Constant Spin", Journal of Spacecraft & Rockets, Vol. 8, No. 1, 1971, pp. 21-27.
7. Kirszenblat, A., "Determination of Allowable Tolerances for Asymmetries of a Free Rolling Missile", Journal of Spacecraft & Rockets, Vol. 11, No. 5, 1974, pp. 295-299.
8.Murphey, C. H. and Bradley, J. W., "Nonlinear Limit Motions of a Slightly Asymmetric Reentry Vehicle" AIAA Journal, Vol. 13, No. 7, 1975, pp. 851-857.
9: Platus, D. H., "Ballistic Reentry Vehicle Flight Dynamics", Journal of Guidance, Control and Dynamics, Vol. 5. No. 1, 1982, pp. 4-16.
10. Etkin, B. *Dynamics of Atmospheric Flight*, John Wiley & Sons Inc., New York, 1972.
11. Murtaugh, S. and Criel, C. H., "Fundamentals of Proportional Navigation" IEEE Spectrum, Dec. 1966, pp. 75-85.
12. Garver, V., "Optimum Intercept Law for Accelerating Targets", AIAA Journal, Vol. 6, No. 11, 1968, pp. 2196-2198.
13. Zarchan, P. *"Tactical and Strategic Missile Guidance"* Chapter 7, American Institute of Aeronautics and Astronautics, Washington DC, 1990.
14. Gutman, S. : "On Optimal Guidance for Homing Missiles", Journal of Guidance and Control, Vol. 3. No. 4, 1979. pp. 296-300.
15. Imado, F. and Miwa, S. "Missile Guidance Algorithm Against High-g Barrel Roll Maneuvers", Journal of Guidance Control and Dynamics, Vol.17. No. 1, 1994, pp. 123-128.

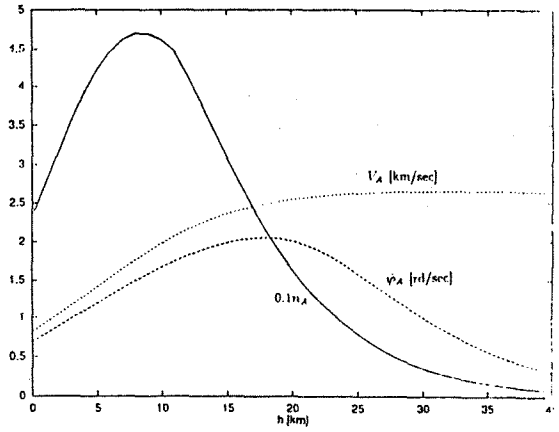

Fig. 1. TBM speed, maneuverabillity and roll rate profile.

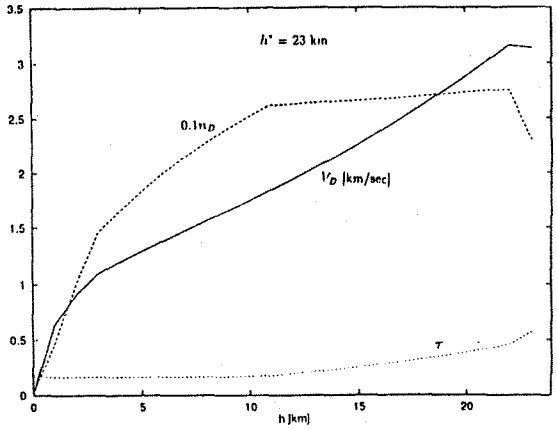

Fig. 2. Interceptor speed, maneuverability and time constant profile ($h^* = 23$ km).

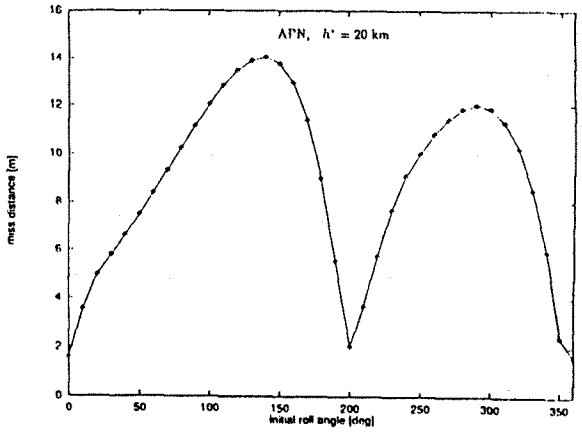

Fig. 3. Miss distance as a function of the initial roll angle (APN, $h^* = 20$ km).

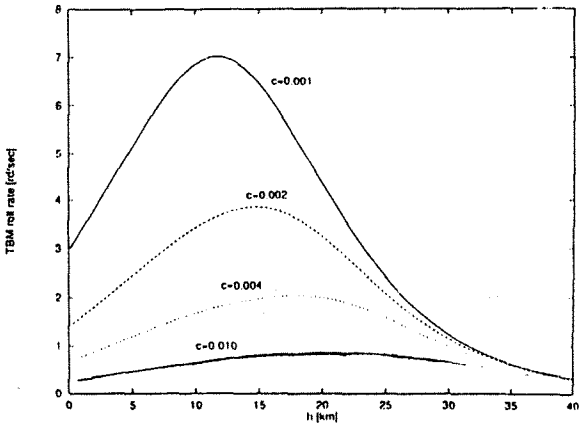

Fig. 4. Roll rate profiles for different roll damping parameters ($c = 3.3\ 10^{-6}$ m/kg).

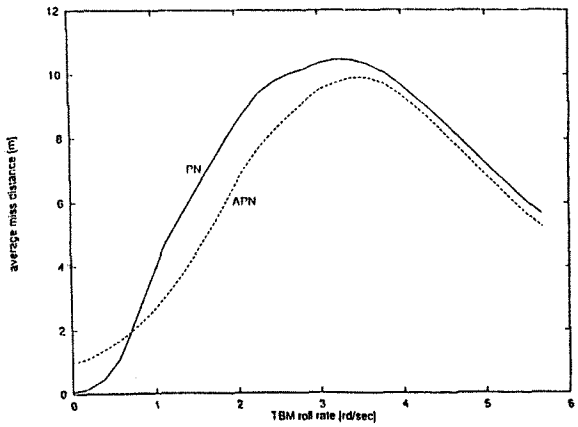

Fig. 5. Average miss distance as function of roll rate (PN & APN, $h^* = 22$ km).

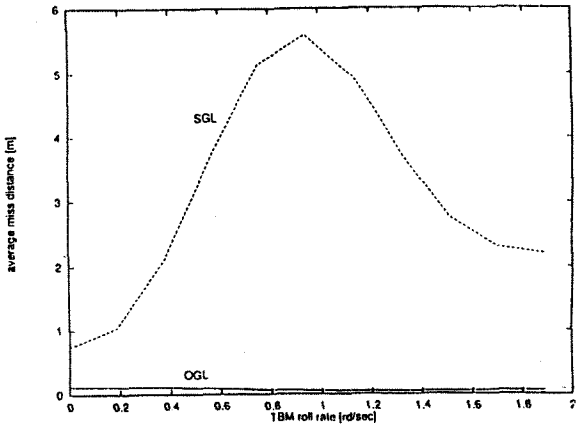

Fig. 6. Average miss distance as function of roll rate (OGL & SGL, $h^* = 22$ km).

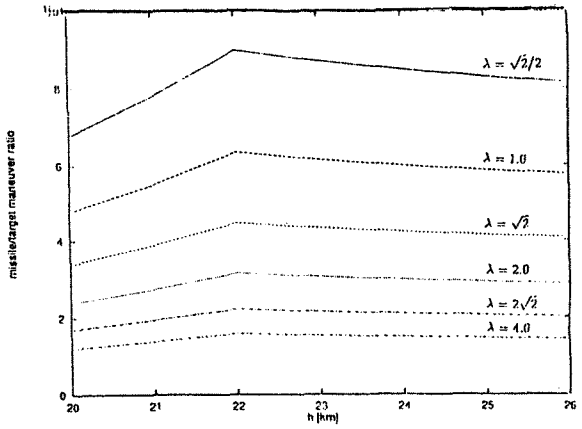

Fig. 7. Missile/target maneuver ratio as function of planned interception altitude.

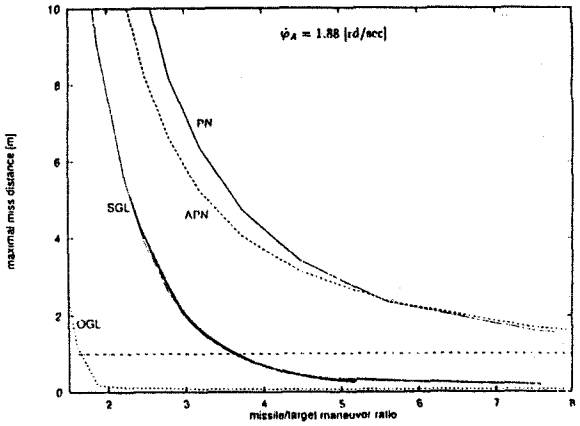

Fig. 8. Maximum miss distance as function of maneuver ratio ($h^* = 22$ km).